PCCP

Accepted Manuscript




ROYAL SOCIETY OF CHEMISTRY

www.rsc.org/pccp

# Doping of Rhenium Disulfide monolayers: A systematic first principles study†

**Deniz Çakır,*[a] Hasan Sahin,[a] and François M. Peeters[a]**

*Received Xth XXXXXXXXXX 20XX, Accepted Xth XXXXXXXXX 20XX*
*First published on the web Xth XXXXXXXXXX 200X*
**DOI: 10.1039/b000000x**

The absence of a direct-to-indirect band gap transition in $ReS_2$ when going from monolayer to bulk makes it special among the other semiconducting transition metal dichalcogenides. The functionalization of this promising layered material emerges as a necessity for the next generation technological applications. Here, structural, electronic, and magnetic properties of substitutionally doped $ReS_2$ monolayers at either S or Re site were systematically studied by using first principles density functional calculations. We found that substitutional doping of $ReS_2$ depends sensitively on the growth conditions of $ReS_2$. Among the large number of non metallic atoms, namely H, B, C, Se, Te, F, Br, Cl, As, P, and N, we identified the most promising candidates for n-type and p-type doping of $ReS_2$. While Cl is an ideal candidate for n-type doping, P appears to be the most promising candidate for p-type doping of $ReS_2$ monolayer. We also investigated the doping of $ReS_2$ with metal atoms, namely Mo, W, Ti, V, Cr, Co, Fe, Mn, Ni, Cu, Nb, Zn, Ru, Os and Pt. Mo, Nb, Ti, and V atoms are found to be easily incorporated in a single layer of $ReS_2$ as substitutional impurity at the Re site for all growth conditions considered in this work. Playing with growth condition energetically makes possible to dope $ReS_2$ with Fe, Co, Cr, Mn, W, Ru, and Os at the Re site. We observe a robust trend for the magnetic moments when substituting a Re atom with metal atoms such that, depending on the electronic configuration of dopant atoms, the net magnetic moment of the doped $ReS_2$ becomes either 0 or 1 $\mu_B$. Among the metallic dopants, Mo is the best candidate for p-type doping of $ReS_2$ owing to favorable energetics and promising electronic properties.

## 1 Introduction

The first experimental realization of graphene triggered a large amount of research efforts on two-dimensional (2D) materials[1–4]. Although graphene is a fascinating material that can be implemented in various technological applications, the absence of an energy band gap inhibits its broader applications. Searching for new 2D materials with promising properties arises as a necessity for developing next generations of electronic devices. Recently, 2D transition metal dichalcogenides (TMD) have been receiving growing attention[5–13]. Unlike graphene, the electronic properties of TMDs range from metal (for instance $NbS_2$) to semiconductor (for instance $MoS_2$).[6] While three dimensional (3D) semiconducting TMDs have an indirect band gap, their 2D monolayers are in general direct band gap materials[5,14,15] with highly desirable optical properties and sufficiently high carrier mobility that have been used to produce e.g. field effect transistors (FETs)[16], logical circuits[17,18] and optoelectronic devices[19–22]. However, the presence of a direct-to-indirect band gap transition limits the applicability of TMDs in, for instance, optoelectronic devices.

Recently, it has been experimentally shown that $ReS_2$ monolayer is a direct gap material with an energy gap of 1.55 eV and the direct-to-indirect gap transition is absent when going from monolayer to bulk.[23] Our experimental and theoretical study on the formation, energetics, and stability of the most prominent lattice defects in monolayer $ReS_2$ have also revealed the tunability of it's characteristic properties upon defect creation.[24] These promising electronic properties of $ReS_2$ make it attractive for optoelectronic device applications. $ReS_2$ prefers to crystallize in a distorted T structure which results in direction dependent electronic properties in $ReS_2$ monolayer. The intrinsic material properties, for instance carrier concentration and mobility, of a material may not be sufficient to fabricate efficient devices. The ability of tuning and manipulating the physical and chemical properties of technologically promising materials are of great importance from both scientific and technological point of views. For instance, the structural imperfections, namely lattice defects (vacancies, adatoms etc.) and impurities (H, C, N etc.), may be exploited to change the electronic, magnetic, and optical properties and chemical reactivity of the materials.

In addition to these unintentional structural imperfections, doping of a material is a well accepted strategy to change its intrinsic physical and chemical properties. In semiconductors, doping is widely employed to tune the carrier density and to adjust the electronic, optical and magnetic properties of semiconductors. Similarly, for 2D semiconductor layered

[a] *Department of Physics, University of Antwerp, 2020 Antwerp, Belgium Fax: +32 3 265 3542; Tel: +32 3 265 3660; E-mail: deniz.cakir@uantwerpen.be*

materials, doping can also be used to control the carrier density. Previous experimental works suggested that doping of $ReSe_2$ with a small amount of Mo and W causes an increase of the carrier concentration, and hence improves their electrical conductivity[25,26]. Furthermore, optical measurements showed that Nb doping results in a small redshift in the energy gap of $ReS_2$[27]. Similar to $ReSe_2$, doping was also used to change the electronic properties of other TMDs such that the electrical conductivity of $MoS_2$ was reported to be modulated by substitutional doping such as Re (leading to n-type doping)[28–30] and Nb (leading to p-type doping)[31,32]. In addition, Au doped $MoS_2$ transistors exhibit a remarkable p-type behavior[33]. Regarding the use of $ReS_2$ in technological applications, a detailed understanding of the dependence of the structural, electronic, and magnetic properties of $ReS_2$ monolayer on different type of structural imperfections is of great importance. In addition to optoelectronic and electronic applications, these 2D materials can be also used in spintronics device applications, requiring doping with magnetic transition metal atoms to create diluted ferromagnetic semiconductors.

In this work we investigated the effect of substitutional doping with nonmetal (H, B, C, Se, Te, F, Br, Cl, As, P, and N) and metal (Mo, W, Ti, V, Co, Cr, Fe, Mn, Ni, Cu, Nb, Zn, Ru, Os, and Pt) atoms on the electronic and magnetic properties of $ReS_2$ monolayer. By using first principles plane wave calculations, we identified suitable dopant atoms for n-type and p-type doping. Additionally, magnetic properties of doped $ReS_2$ were also studied to discuss the possibility of using doped-$ReS_2$ in spintronics applications.

## 2 Computational Methodology

First principle calculations were carried out in the framework of density functional theory (DFT) as implemented in the Vienna ab initio simulation package (VASP)[34,35]. The generalized gradient approximation (GGA) within Perdew-Burke-Ernzerhof (PBE) formalism was employed for the exchange-correlation potential[36]. The projector augmented wave (PAW) method[37] and a plane-wave basis set with an energy cutoff of 500 eV were used in the calculations. A 2×2 supercell containing 48 atoms was used to study the structural, electronic, and magnetic properties of doped $ReS_2$ monolayer. Brillouin zone integration was performed using a regular 3×3×1 k-mesh within the Monkhorst-Pack scheme. Density of states calculations were performed on a 7×7×1 k-mesh[38]. Gaussian smearing method was employed and the width of the smearing was chosen as 0.05 eV. Lower smearing values (0.005 eV) were used to obtain the correct spin configurations in the relaxed structures. The convergence criterion of the self consistent field calculations was set to $10^{-5}$ eV for the total energy. To prevent spurious interaction between isolated $ReS_2$ monolayers, a large vacuum spacing (at least 12 Å) was introduced. By using the conjugate gradient method, atomic positions and lattice constants were optimized until the atomic forces are less than 0.01 eV/Å. Pressure on the supercells was decreased to values less than 1 kB. Before studying doping properties of the $ReS_2$ monolayer, we first calculated the substitution energy for the substitutional doping with representative atoms (Cl atom at S site and with Nb atom at Re site) as a function of supercell size. When going from 2×2 cell (containing 48 atoms) to 4×4 cell (containing 192 atoms), the change in the substitution energy is in the order of meV. These results show that a 2×2 super cell is enough to investigate doping of the $ReS_2$ monolayer. The present computational setup predicts a band gap of 1.43 eV for $ReS_2$ monolayer, being very close to the experimental gap of 1.55 eV[23].

The substitution energy of a particular dopant atom at either S or Re site is obtained by using the following expression,

$$E_{subs} = E_{tot}[ReS_2 + D] - E_{tot}[ReS_2] + \mu_{S(Re)} - \mu_D$$

where $E_{tot}$[$ReS_2$+D] is the total energy of the $ReS_2$ monolayer with substitutional dopant $D$, $E_{tot}$[$ReS_2$] is the total energy of a pristine $ReS_2$ monolayer, while $\mu_{S(Re)}$ and $\mu_D$ are the chemical potentials of the substituted atom (S or Re) in the host lattice and the dopant atom, respectively. The chemical potentials of O, F, H, Cl and Br are set to half the total energy of their respective gas phases (i.e., $D_2$). For the rest of the dopants, the bulk phase of each element is chosen to determine the chemical potentials. At equilibrium, the stability of $ReS_2$ can be studied by calculating the heat of formation as

$$2\mu_S + \mu_{Re} = \mu_{ReS_2} = 2\mu_S^{bulk} + \mu_{Re}^{bulk} - \Delta H_f$$

where $\Delta H_f$ is the heat of formation and is found to be -1.75 eV. Here $\mu_{ReS_2}$ is set to the total energy of the pristine monolayer. It is well known that the value of the chemical potentials are largely determined by the specific experimental conditions. In this study, we consider two limiting cases, namely Re and S-rich situations. For the Re-rich condition, the chemical potential of Re was taken from bulk Re (i.e. $\mu_{Re}$=$E_{tot}$[bulk Re]) and by using $\mu_S$ = 1/2 ($E_{tot}$[$ReS_2$])-$E_{tot}$[Re bulk]) we determined the chemical potential of S. Similarly, for the S-rich condition, the S chemical potential is equal to the its bulk value and, at this condition, Re chemical potential was obtained via $\mu_{Re}$= $E_{tot}$[$ReS_2$]-2$E_{tot}$[S bulk].

## 3 Single Layer Rhenium Disulfide

Monolayer $ReS_2$ is the most recently synthesized member of the semiconductor TMDs. Although most of the well-known TMDs with chemical formula $MX_2$ (M= Mo, W, V, Ta, Hf and X= S, Se) are in 1H or 1T phase in their ground state, the atomic structure of $ReS_2$ single layers have neither H nor T

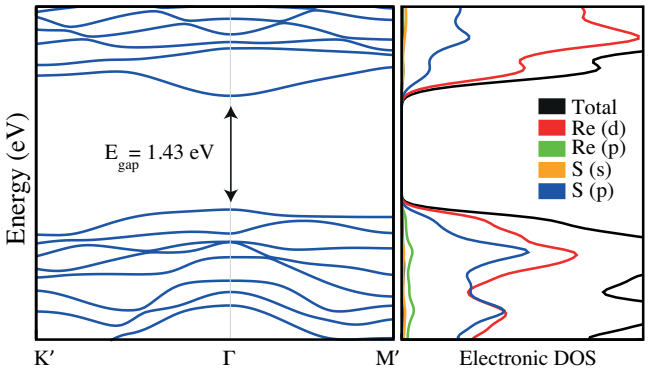


**Fig. 1** (Color online) Electronic band dispersion and the orbital decomposed electronic density of states of single layer $ReS_2$.

character. As it was reported before[23,24] $ReS_2$ crystallizes in a distorted-1T structure with forming parallel Re chains along the van der Waals plane. In Fig. 1, we present the electronic band dispersion and the orbital decomposed electronic density of states of single layer $ReS_2$. As we reported before single layer $ReS_2$ is a semiconductor with a direct band gap (1.43 eV) at the Γ high symmetry point.[23,24] Both the valence band maximum and the conduction band minimum occur at the Γ symmetry point. Due to the distorted hexagonal lattice symmetry we use the high symmetry points as $K'$ and $M'$. Here it is worth to note that for crystal structures having distorted lattice symmetry electronic band dispersion may miss some states. Therefore, it is more convenient to discuss energy band gap by density of states (DOS). It appears from partial DOS (PDOS) analysis shown in Fig. 1 that both the valence and conduction band edges are mainly composed of Re-*d* and S-*p* states. We also see that hybridization of Re-*s*, Re-*p* and S-*s* states with bonding and anti-bonding states are negligible.

## 4 Substitution at the S site

### 4.1 Stability and Energetics

The calculated substitution energies of metal and nonmetal dopant atoms at S site at both Re- and S-rich conditionals are listed in Tables 1 and 2. Due to the distorted T structure, several different S sites on the $ReS_2$ monolayer are possible for the replacement of S by dopant atoms, which are denoted in Fig. 2. As seen in Tables 1 and 2, the favorable site for the substitution is not the same for all atoms and are largely dependent on the electronic configuration and the size of the dopant atom. B, C, N, and H have a smaller atomic size when compared to the rest of the nonmetallic dopant atoms, and therefore prefer to occupy site I. F, Cl, Br, Se, Te, and As atoms favor bonding on site VI where dopant atoms have more space available to reside. Site VI is also found to be the most favor-

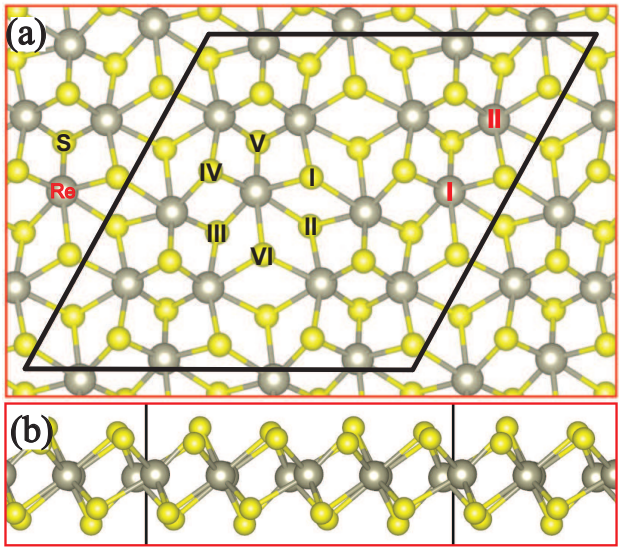


**Fig. 2** (Color online) Top (a) and side (b) views of the optimized structure of the 2×2 supercell (enclosed by the black lines) used in the calculations. The different S and Re sites for substitutional doping are indicated by black and red numbers, respectively. Structures are prepared using the VESTA program.[39]

**Table 1** Calculated magnetic moment ($\mu$) in units of $\mu_B$, the substitution energy ($E_{subs}$) in eV under S-rich ($E_{subs,S}$) and Re-rich ($E_{subs,Re}$) conditions and the most favorable substitution at the S site.

| dopant | $\mu$ | $E_{subs,S}$ | $E_{subs,Re}$ | site |
|---|---|---|---|---|
| H | 1.00 | 2.089 | 1.242 | I |
| B | 1.00 | 2.772 | 1.925 | I |
| C | 0.00 | 3.129 | 2.282 | I |
| N | 1.00 | 2.085 | 1.238 | I |
| P | 1.00 | 1.245 | 0.399 | V |
| As | 1.00 | 1.799 | 0.952 | VI |
| O | 0.00 | -0.915 | -1.761 | VI |
| Se | 0.00 | 1.377 | 0.531 | VI |
| Te | 0.00 | 0.847 | 0.001 | I |
| F | 1.00 | -0.953 | -1.800 | VI |
| Cl | 0.00 | 0.942 | 0.095 | VI |
| Br | 0.00 | 1.320 | 0.473 | VI |

**Table 2** Calculated magnetic moment ($\mu$) in units of $\mu_B$, the substitution energy ($E_{subs}$) in eV under S-rich ($E_{subs,S}$) and Re-rich ($E_{subs,Re}$) conditions and the most favorable substitution at the S site.

| dopant | $\mu$ | $E_{subs,S}$ | $E_{subs,Re}$ | site |
|---|---|---|---|---|
| Ti | 0.00 | 2.083 | 1.236 | I |
| V | 1.00 | 2.979 | 2.132 | I |
| Cr | 4.00 | 3.508 | 2.661 | VI |
| Mn | 3.00 | 2.669 | 1.822 | VI |
| Fe | 2.00 | 3.177 | 2.330 | VI |
| Co | 1.00 | 3.149 | 2.299 | VI |
| Ni | 0.00 | 2.233 | 1.386 | VI |
| Cu | 1.00 | 2.810 | 1.963 | VI |
| Zn | 0.00 | 2.589 | 1.742 | VI |
| Nb | 0.00 | 3.612 | 2.766 | I |
| Mo | 2.00 | 4.389 | 3.542 | I |
| W | 2.00 | 5.268 | 4.421 | I |
| Pt | 0.00 | 1.777 | 0.930 | VI |

able site to create a S vacancy. The creation of a S vacancy at site V, which is preferred by P atoms, is highly unfavorable. For P, the difference in substitution energy between site V and site VI is about 0.23 eV. We observed that there is a strong correlation between the $E_{subs}$ values and the bulk/molecular cohesive energy values of the dopant atoms in each row of the periodic table. $E_{subs}$ decreases when going from left to right in the periodic table. C is the strongest material in bulk form, and thus leads to the largest positive substitution energy amongst the nonmetallic elements. $E_{subs}$ for the S site is positive and large for most of the elements studied in this work. Positive values indicate that dopant atoms are unlikely to be incorporated into the $ReS_2$ monolayer. We found that $E_{subs}$ is negative for O and F atoms, indicating the spontaneous formation of substitutional doping at S site for these dopant atoms.

Similar to $ReS_2$, $ReSe_2$ also has a distorted T structure with a slightly larger unit cell[41]. Thus, one can expect a negative $E_{subs}$ for Se doping. Interestingly, the replacement of a S by either a Se or a Te atom is endothermic and, one needs to supply more energy in order to incorporate a Se atom into the $ReS_2$ monolayer. This clearly implies that the formation of the mixed $ReS_{2-x}Te_x$ alloy is energetically more likely as compared to that of $ReS_{2-x}Se_x$. Adversely, it has been shown that the mixing energy for $MoS_2/MoSe_2$ ($MoS_2/MoTe_2$) is always negative (positive)[42]. In other words, S-Se alloys are thermodynamically stable. In this previous theoretical work, the mixing energies were calculated by using

$$E_{mix} = E_{tot}[A_xB_{1-x}] - (xE_{tot}[A] + (1-x)E_{tot}[B])$$

where $E_{tot}[A_xB_{1-x}]$ is the total energy of the mixed compound, while $E_{tot}[A]$, and $E_{tot}[B]$ are the total energies of the constitute compounds, respectively. $x$ is the relative concentration of the chalcogen atoms. If the same definition is used to calculate the mixing energy of $ReS_2$ and $ReSe_2$ compounds for low Se concentrations, $E_{mix}$ is found to be negative (-0.01 eV), indicating the stability of mixed S-Se alloys over segregated phases even at 0 K. Indeed, our results are in a good agreement with a previous work that shown the presence of the stable mixed S-Se layer compounds[40]. In the case of mixed S-Te alloys, the mixing of two phases ($ReS_2$ and $ReTe_2$) is unlikely with a positive $E_{mix}$ value of 0.12 eV at $x$=0.97. While $ReTe_2$ does not form a layer structure in its bulk form[43], we first assumed that $ReTe_2$ has the same crystal structure as $ReS_2$ in the total energy calculations. If we include the entropy contribution (which promotes random distribution) by using $S$=$-2[xlnx+(1-x)ln(1-x)]k_B$, the free energy of the mixing (i.e. $E_{mix}$ - $TS$) for the Te case is found to be still positive with a value of 0.11 eV at room temperature. Considering the experimentally observed bulk structure of $ReTe_2$, $E_{mix}$ becomes even more positive and does not change our conclusion. Since these S-Se and S-Te alloy compounds are not the scope of this work, we just calculated $E_{mix}$ for a few low Se and Te concentrations. In other words, $x$ was taken very close to unity. While we considered bulk Se and Te as references for our $E_{subs}$ calculations, $E_{mix}$ reflects the thermodynamical stability of mixed S-Se and S-Te alloys relative to separated $ReS_2$, $ReSe_2$ and $ReTe_2$ compounds. Since the bulk phase of Se is more stable than that of Te in terms of their bulk cohesive energy values, it is understandable that Te doping of $ReS_2$ is easier relative to Se doping.

To get more insight into mixed S-Se and S-Te alloys, we also investigated the clustering energy of two Se and two Te atoms. While Se atoms do not prefer a particular configuration, Te atoms tend to stay close to each other. In the Te case, when one places two Te atoms as far apart as possible, the energy difference between this configuration and the lowest energy configuration is 86 meV in favor of clustering. In other words, Te atoms favor the short-range ordering in mixed S-Te alloys. For the Se case, the energy difference between the different configurations is at most only 18 meV. This means that the formation of random S-Se alloys is possible. Moreover, $E_{mix}$ becomes even more negative (-0.03 eV) for the two Se atoms corresponding to $x$=0.94. Our calculations suggest that random S-Se alloys could be fabricated by appropriate techniques, for instance by using chemical vapor deposition.

In contrast to nonmetallic dopants, metal atoms generally have much larger positive $E_{subs}$ values summarized in Table 2, which indicates that the separated phases of the bulk form of the metal dopants and $ReS_2$ monolayer are thermodynamically more stable than the metal doped $ReS_2$ monolayer.

### 4.2 Electronic and Magnetic properties of nonmetal atom doped $ReS_2$

The effect of doping on the electronic properties of a $ReS_2$ monolayer is examined by partial density of states (PDOS) calculations, shown in Fig. 3. Since the substitutional doping at S site with transition metal atoms is quite unlikely as compared to that with nonmetal atoms, we just focused on the electronic properties of nonmetal atom doped $ReS_2$ monolayer. It is clear that except isoelectronic atoms (O, Se, and Te), dopant atoms induce localized states within the gap of bare $ReS_2$. B, N, P, and As may result in p-type doping of the $ReS_2$ monolayer, since these atoms have less $p$ electrons as compared to the S atom. In the case of N doping, both spin up and spin down channels appear above the valence band maximum (VBM), and these states are mainly formed by hybridization between N $2p$ and Re $5d$ states with a small contribution from the $3p$ states of the nearest S atoms. B-doped $ReS_2$ has a similar PDOS with a slightly smaller spin splitting relative to N-doped $ReS_2$ monolayer. For P doping, spin-slitting becomes even smaller and the defect states move closer to VBM of $ReS_2$. For As substitution, while the spin up state moves even more towards the VBM, the spin down state moves away from the VBM, leading to an increased in spin splitting. C doping induces a deep defect level within the band gap of $ReS_2$. Among the dopants investigated here, P appears as the most promising impurity for p-type doping of $ReS_2$, since impurity states are very close to the VBM. O, Se, and Te are isoelectronic to S and thus lead to only minor changes in the electronic properties of $ReS_2$ monolayer. The direct band gap of the $MoS_2$ monolayer has been shown to be tuned by changing the Se concentration in the mixed S-Se random alloys, which is useful for optoelectronic applications[42]. Similarly, such method may also be used in the case of $ReS_2$. Halogen atoms (F, Cl, and Br) and H atoms serve as an electron donor to the $ReS_2$ monolayer. F and H doped $ReS_2$ monolayer has a magnetic ground state with a net magnetic moment of 1 $\mu_B$. Differing from the other nonmetallic dopants, the H atom only binds to two neighboring Re atoms with an average binding distance of 1.90 Å, resulting in a non-bonding Re atom. The hybridization of the H $s$ orbital with $d$ orbitals of Re atoms and non-bonded Re atom gives rise to several defect states localized within the band gap of pristine $ReS_2$. In the case of F, an occupied (empty) minority (majority) defect state appears 0.35 (0.14) eV below the conduction band minimum (CBM). These defect states originate from the hybridization of F $3p$ and Re $5d$ states with a small contribution from the neighboring $p$ states of the S atoms. Although Br and Cl are expected to result in a magnetic ground state, the spin polarized and spin-unpolarized states are almost degenerate with an energy difference of 2-3 meV (such difference is 28 meV for F doping) in favor of a magnetic state with a net magnetic moment of 1

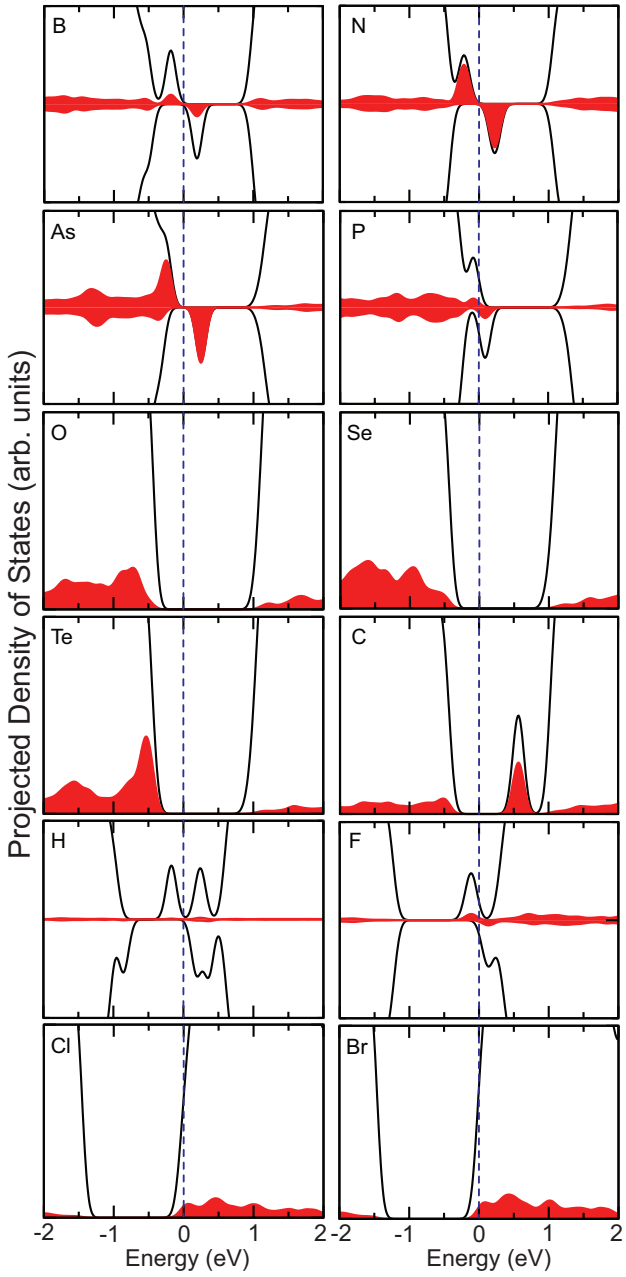


**Fig. 3** (Color online) Density of states of B, N, As, P, O, Se, Te, C, H, F, Cl, and Br substituted $ReS_2$. PDOS for dopant atoms are denoted by red curves. Black curves represent the total DOS. For the magnetic systems PDOS of spin up and spin down (plotted as negative PDOS) electrons are given separately. Vertical blue dashed lines show the Fermi level. The PDOS of the dopant atoms is enlarged in order to make them visible.

$\mu_B$. However, at finite temperatures, for instance at room temperature, it is easily foreseen that only the nonmagnetic state can survive due to fluctuations in the system. Therefore, it is more meaningful to investigate the spin-unpolarized state for the possible device applications. Since Br and Cl atoms have one extra $p$ electron with respect to S, they donate this electron into the conduction band of the $ReS_2$, leading to n-type doping. This finding clearly indicates that these halogen atoms act as an ideal source for n-type doping. While $E_{subs}$ is large and positive for Br, Cl has a slightly positive $E_{subs}$ under Re-rich condition. Hence, Cl appears as a much better candidate for n-type doping of $ReS_2$ monolayer. Recently, it has been shown that a field effect transistor made of Cl-doped $MoS_2$ exhibits a much better performance (i.e., a much lower contact resistance) as compared to that of clean $MoS_2$ [44]. Cl doping results in an upward shift of the Fermi level, which suggests an n-type doping of $MoS_2$. A common observation valid for most of the nonmetal dopant atoms: when the atomic number of the dopant atoms increases, the spin splitting decreases and, the corresponding defect states move towards either VBM or CBM depending on the type of dopant atom.

The replacement of a S atom by metallic and nonmetallic dopant atoms also modifies the magnetic properties of the bare $ReS_2$ monolayer. While $ReS_2$ monolayer doped with H, B, N, F, P, and As have a magnetic ground state with a net magnetic moment of 1 $\mu_B$, C, O, Se, and Te doping results in a nonmagnetic ground state. About half of the total magnetization in the B case comes from a neighboring Re atom. For F, B and P doping, the main part of the total magnetization stems from several neighboring Re atoms. N and As have a somewhat different behavior. They almost carry one third of the total magnetization. Re atoms bonded to an H atom significantly contributes to the total magnetization in H doped $ReS_2$. Together with S, Se, Te, and O belong to chalcogens and they are isoelectronic to each other. Thus, the replacement of S by Se, Te, and O does not induce any magnetic properties. The magnetism in Cu doped $ReS_2$ mainly comes from the neighboring S and Re atoms. Zn has $s^2d^{10}$ electronic configuration. Our charge analysis shows that 4$s$ electrons of Zn are transferred to the $ReS_2$ monolayer, occupying the Re 5$d$ orbitals. This leads to a nonmagnetic ground state in Zn doped $ReS_2$ monolayer. In the case of metal atoms, which have partially filled $d$ states, when we substitute the S atoms, we get somewhat higher magnetic moments depending on the electronic structure of the metal atom. For 3$d$ metals, the magnetic moments follow a trend that is observed for isolated transition metal atoms. The magnetic moment increases from Ti to Cr, and takes the largest value of 4 $\mu_B$ for Cr. Starting from Mn, it decreases and becomes 0 $\mu_B$ for Ni. The spin polarization in magnetic systems is mostly localized on the metal atoms. Nevertheless, due to the spatial extension of the spin density, neighboring Re atoms also make a relatively small contribution ($\sim$ 0.10-0.25 $\mu_B$ in the minority spin channel) to the total magnetization.

**Table 3** Calculated magnetic moment ($\mu$) in units of $\mu_B$, the substitution energy ($E_{subs}$) in eV under S-rich ($E_{subs,S}$) and Re-rich ($E_{subs,Re}$) conditions and the most favorable substitution at the Re site.

| dopant | $\mu$ | $E_{subs,S}$ | $E_{subs,Re}$ | site |
|---|---|---|---|---|
| Ti | 1.00 | -2.826 | -1.086 | I |
| V | 0.00 | -2.155 | -0.415 | I |
| Cr | 1.00 | -1.512 | 0.228 | I |
| Mn | 0.00 | -1.529 | 0.211 | I |
| Fe | 1.00 | -0.710 | 1.030 | I |
| Co | 0.00 | -0.208 | 1.532 | I |
| Ni | 1.00 | 0.571 | 2.311 | I |
| Cu | 0.00 | 1.501 | 3.241 | I |
| Zn | 1.00 | 1.027 | 2.757 | I |
| Nb | 0.00 | -2.593 | -0.854 | I |
| Mo | 1.00 | -1.886 | -0.146 | I |
| W | 1.00 | -1.674 | 0.066 | I |
| Os | 1.00 | -0.423 | 1.317 | I |
| Ru | 1.00 | -0.804 | 0.936 | I |
| Pt | 1.00 | 0.895 | 2.635 | I |

**Table 4** $E_{subs,closest}$ and $E_{subs,farthest}$ (for S-rich condition) stands for the substitution energies when the metal atoms stay close to each other and isolated, respectively. Pairing energy ($\Delta E$=$E_{subs,closest}$-$E_{subs,farthest}$) is also given in eV.

| dopant | $E_{subs,closest}$ | $E_{subs,farthest}$ | $\Delta E$ |
|---|---|---|---|
| Fe | -2.378 | -1.502 | -0.875 |
| Ti | -5.907 | -6.085 | 0.179 |
| Nb | -5.104 | -5.283 | 0.179 |
| Mn | -3.214 | -3.069 | -0.145 |
| W | -3.616 | -3.345 | -0.271 |
| Mo | -3.948 | -3.773 | -0.175 |

## 5 Substitution at the Re site

### 5.1 Stability and Energetics

Here, we investigated all possible different Re sites for substitution, denoted by the red symbols in Fig. 2. We considered transition metal atoms, namely Mo, W, Ti, V, Cr, Fe, Co, Mn, Ni, Cu, Nb, Zn, Os, Ru and Pt, to substitute Re. Table 3 summarizes the induced magnetic moments, $E_{subs}$ for both S- and Re-rich conditions, and the most favorable substitution site. We found a clear trend in the $E_{subs}$ values i.e. $E_{subs}$ decreases with increasing occupancy of $d$ orbitals in each row of the periodic table. Since the formation of Re vacancies is easier at site I as compared to site II, all metal atoms prefer to occupy

site I. Ti, V, Nb, and Mo have large and negative $E_{subs}$ for both S- and Re-rich conditions, indicating thermodynamical stability of the substitution. The S-rich limit is more appropriate to dope $ReS_2$ monolayer with Fe, Cr, Co, Mn, W, Os, and Ru atoms as compared to the Re-rich limit, since $E_{subs}$ becomes negative in the former. As seen in Table 3, $E_{subs}$ is large and positive for Cu, Pt, Zn, and Ni atoms and thus these transition metal atoms are not suitable candidates for doping of $ReS_2$. Interestingly, metal atoms having less valence electrons than Re are found to be most promising candidates for substitutional doping of $ReS_2$ in terms of energetics.

Our results clearly show that $E_{subs}$ strongly depends on the chemical potentials of the Re and S atoms. The substitution at S (Re) site becomes much more easy when the $ReS_2$ monolayer is grown under S (Re) poor condition. This means that in order to get substitutional doping at the S (Re) site we should first fabricate $ReS_2$ at the S (Re)-poor condition and then the resultant S (Re) vacancies can be filled with appropriate dopant atoms. This strategy was also suggested for doping of $MoS_2$ [45].

Next, for Mn, Fe, W, Nb, W, and Ti atoms, we also calculated the pairing energy ($\Delta E$) of two dopant atoms. $\Delta E$ is the substitution energy difference between two different arrangements of dopant atoms on the $ReS_2$ monolayer. While the metal atoms are placed at nearest neighboring positions in the first configuration, they are placed as far as possible in the second one. Negative $\Delta E$ means that metal atoms prefer to stay as close as possible. We found that Mn, Fe, Mo, and W atoms prefer to cluster in the $ReS_2$ monolayer while Ti and Nb atoms tend to stay isolated, see Table 4. However, migration of dopant atoms is quite unlikely and therefore clustering of dopants is hampered by the large energy barriers. While Cu, Zn, Ni and Pt atoms prefer to occupy the S site in the Re-rich condition, the Re site becomes energetically more favorable for the S-rich condition. In a recent work, it was shown that substituting Mo with Au in $MoS_2$ is highly unfavorable, confirming our finding that nobel metal atoms prefer to stay at the S site under certain conditions [46].

In addition to the metal dopants, we also calculated the pairing energy for Cl and P atoms at the S-poor condition for comparison. While P atoms prefer to avoid each other and to stay isolated with a large $\Delta E$ of 0.45 eV, Cl atoms do not have a clear preference with a $\Delta E$ of about 0.01 eV. More importantly, $E_{subs}$ becomes -0.13 eV for the Cl case, suggesting that the doping of $ReS_2$ with Cl is quite favorable in terms of energetic.

### 5.2 Electronic and Magnetic properties of transition metal atom doped $ReS_2$

We discuss the electronic properties of the transition metal atom doped $ReS_2$ monolayer by calculating PDOS, shown in

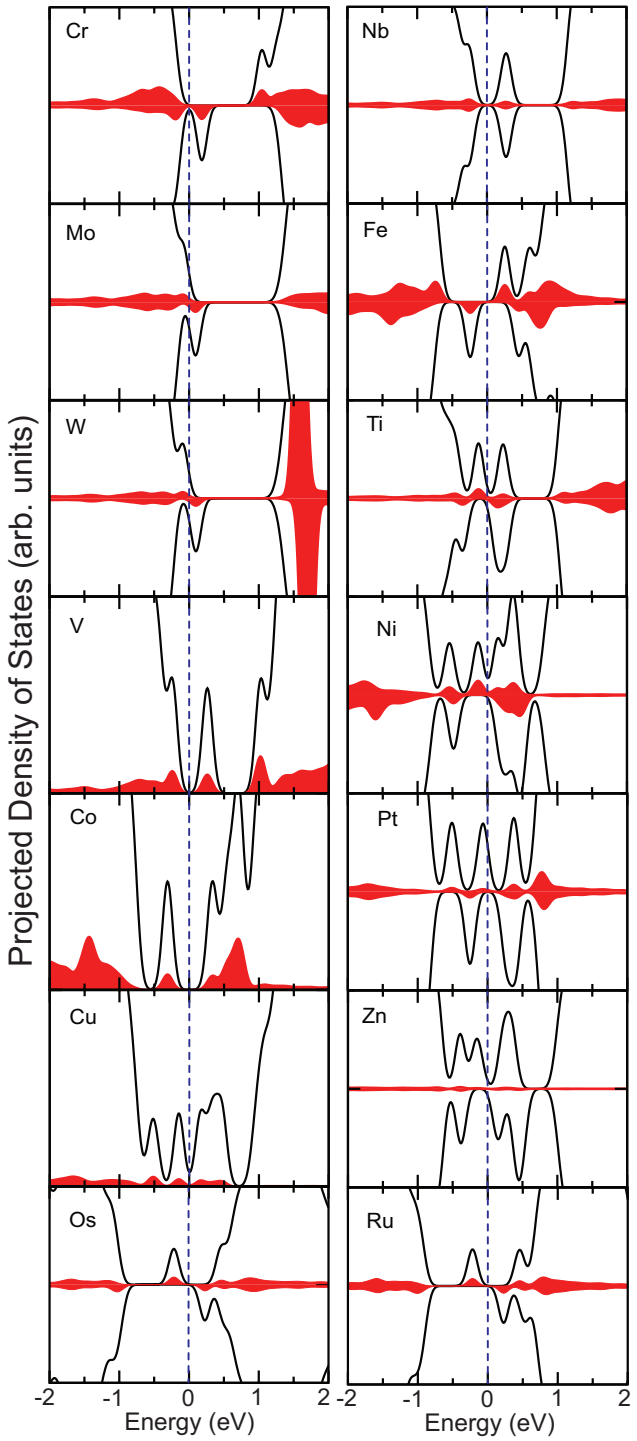


**Fig. 4** (Color online) Density of states for substitutional doping at Re site with Cr, Nb, Mo, Fe, W, Ti, V, Ni, Co, Pt, Cu, Zn, Os, and Ru atoms. PDOS of dopant atoms are denoted by red curves. Black curves represent the total DOS. Vertical blue dashed lines show the Fermi level. For the magnetic systems PDOS of spin up and spin down (plotted as negative PDOS) electrons are given separately.

Fig. 4. As expected Ti, V, Cr, Mo, Nb and W, which have less valence electrons than Re, result in p-type doping of $ReS_2$. Mo is found to be the best candidate for p-type doping of $ReS_2$, since the associated defect levels are very close to the VBM and $E_{subs}$ is negative for both Re- and S-rich conditions. This result indicates that incorporation of Mo into $ReS_2$ leads to the formation of impurity levels, which causes an increase of the electrical conductivity by increasing the carrier density and thus leads to a significant drop in the carrier activation energy. W-doping also seems to be attractive. However, while W has a PDOS quite similar as Mo, $E_{subs}$ is positive for the Re-rich condition, limiting the usage of W for p-type doping of $ReS_2$. In the Mo doping case, while the majority spin state appears at the top of the VBM, the minority spin state is at 0.1 eV above the VBM. Unlike Mo and W, Cr doping induces a defect state 0.25 eV above the VBM. This defect state moves closer to VBM in the case of Mo and W doping. Previous calculations on Nb doped $MoS_2$ indicated that Nb is a promising transition metal for p-type doping. However, in the case of $ReS_2$, Nb substituting Re creates a deep acceptor defect state at 0.5 eV above the VBM. Although Ti and V doping at Re site are quite favorable in terms of energetics, the resultant electronic structure of the doped $ReS_2$ is not efficient for p-type doping. When Fe, Pt, Cu, Co, and Ni atoms substitute a Re atom, several gap states are formed. The number of gap states increases when the dopant atoms have a $d$-orbital occupancy larger than Re. The Fermi level moves deeper into the gap of the $ReS_2$ as the occupancy of $d$ orbitals increases. In spite of the favorable $E_{subs}$ in the S-rich condition, Fe and Co are not good candidates neither for n-type nor for p-type doping, since the Fermi level lies within the band gap of $ReS_2$, and thus associated defect levels are far away from both VBM and CBM, thereby resulting in larger carrier activation energies as compared to Mo and W-doped $ReS_2$. Mn and Re are isoelectronic to each other. Therefore, PDOS of Mn-doped $ReS_2$ (not shown) has no gap states and is similar to that of pristine $ReS_2$. Interestingly, in contrast to nonmetal dopants which may result in both n- and p-type doping, an efficient n-type doping of $ReS_2$ is not achieved for the transition metal atoms investigated in this work.

Except Cu, Pt, V, Co and Nb, the rest of the transition metal atoms result in a magnetic ground state with a net magnetic moment of 1 $\mu_B$. We obtained a strong trend in magnetic moments which becomes either 0 or 1 in each row of the periodic table. Therefore, we propose a simple electron counting rule to explain the observed trend in magnetic moments. When the sum of valence electrons of Re and dopant atoms is an odd number (resulting in an unpaired electron), the net magnetic moment becomes 1 $\mu_B$. This simple explanation clearly shows that one can easily foresee the total magnetic moment of the metal doped-$ReS_2$ monolayer without having to perform calculation or experiment. The energy difference between the spin polarized and spin unpolarized states in magnetic systems ranges from 24 meV for Mo to 133 meV for Fe, implying the stability of the ferromagnetic state at fairly high temperatures. Depending on the electronic structure, each dopant atom contributes differently to the total magnetization. For Fe doping, Fe atom carries more than half of the total magnetization (0.59 $\mu_B$), and a considerable part of the magnetization (0.42 $\mu_B$) is localized on a neighboring Re atom. Ti exhibits completely distinct behavior such that the magnetization is distributed over several neighboring S atoms, and especially the Re atoms significantly contribute to the total magnetization. Since Zn has filled $s$ and $d$ shells, the magnetization mainly originates from the neighboring Re and S atoms, while the contribution from Zn atoms is found to be negligible. In the case of Mo and W, in addition to the dopant atoms (about 0.23 $\mu_B$ for Mo and 0.15 $\mu_B$ for W), several neighboring Re and S atoms contribute to the total magnetization. When we dope with two transition metal atoms, we checked all possible magnetic orderings, namely ferromagnetic (FM), anti-ferromagnetic (AFM), and non-magnetic. Our calculations revealed that while singly doped $ReS_2$ exhibits magnetism for Fe, Ti, Mo, and W, doubly doped $ReS_2$ monolayer has a nonmagnetic ground state in the lowest energy configuration, shown in Table 4. For doubly Mn-doped $ReS_2$, the FM state with a net magnetic moment of 2 $\mu_B$ and the AFM state are almost degenerate.

## 6 Conclusions

We investigated the electronic and magnetic properties of $ReS_2$ monolayer substitutionally doped by transition metal and nonmetal atoms. The substitutional doping of $ReS_2$ is largely dependent on the growth conditions of the $ReS_2$ monolayer. By choosing proper experimental conditions, we predict that various dopants can be easily incorporated into the $ReS_2$ monolayer. The formation energies for O and F have large negative values, indicating thermodynamical stability for substitution. Among nonmetal dopant atoms, Cl is found to be the best candidate for n-type doping. Due to the very high $E_{subs}$, the replacement of S by metal atoms is unlikely. In contrast, transition metal atom doping at the Re site seems to be efficient and easy when compared to nonmetal atom doping at the S site since $E_{subs}$ is easily switched between negative and positive values by changing the growth condition. Mo, Fe, Cr, Nb, W, and Ti have negative $E_{subs}$ under Re-poor condition. Mo is the most promising candidate for p-type doping of the $ReS_2$ monolayer.

This work was supported by the Flemish Science Foundation (FWO-Vl) and the Methusalem foundation of the Flemish government. Computational resources were provided by TUBITAK ULAKBIM, High Performance and Grid Computing Center (TR-Grid e-Infrastructure), and HPC infrastructure of the University of Antwerp (CalcUA) a division of the

Flemish Supercomputer Center (VSC), which is funded by the Hercules foundation. H.S. is supported by a FWO Pegasus-long Marie Curie Fellowship. D.C. is supported by a FWO Pegasus-short Marie Curie Fellowship.

## References


1 K. S. Novoselov, A. K. Geim, S. V. Morozov, D. Jiang, S. C. Dubonos, I. V. Grigorieva, and A. A. Firsov, Science, 2004, **306**, 666.

2 A. K. Geim and K. S. Novoselov, Nat. Mater., 2007, **6**, 183.

3 A. H. C. Neto, F. Guinea, N. M. R. Peres, K. S. Novoselov, and A. K. Geim, Rev. Mod. Phys., 2009, **81**, 109.

4 S. D. Sarma, S. Adam, E. H. Hwang, and E. Rossi, Rev. Mod. Phys., 2011, **83**, 407.

5 K. F. Mak, C. Lee, J. Hone, J. Shan, and T. F. Heinz, Phys. Rev. Lett., 2010, **105**, 136805.

6 C. Ataca, H. Sahin, and S. Ciraci, J. Phys. Chem. C, 2012, **116**, 8983.

7 Q. H. Wang, K. Kalantar-Zadeh, A. Kis, J. N. Coleman, and M. S. Strano, Nat. Nanotechnol., 2012, **7**, 69917712.

8 X. Song, J. Hu, and H. Zeng, J. Mater. Chem. C, 2013, **1**, 2952.

9 M. Xu, T. Liang, M. Shi, and H. Chen, Chem. Rev., 2013, **113**, 3766.

10 X. Huang, Z. Zeng, and H. Zhang, Chem. Soc. Rev., 2013, **42**, 1934.

11 M. Chhowalla, H. S. Shin, G. Eda, L.-J. Li, K. P. Loh, and H. Zhang, Nat. Chem., 2013, **5**, 26317275.

12 S. Horzum, H. Sahin, S. Cahangirov, P. Cudazzo, A. Rubio, T. Serin, and F. M. Peeters, Phys. Rev. B, 2013, **87**, 125415.

13 H. Sahin, S. Tongay, S. Horzum, W. Fan, J. Zhou, J. Li, J. Wu, and F. M. Peeters, Phys. Rev. B, 2013, **87**, 165409.

14 A. Kuc, N. Zibouche, and T. Heine, Phys. Rev. B, 2011, **83**, 245213.

15 W. S. Yun, S. W. Han, S. C. Hong, I. G. Kim, and J. D. Lee, Phys. Rev. B, 2012, **85**, 033305.

16 B. Radisavljevic, A. Radenovic, J. Brivio, V. Giacometti, and A. Kis, Nat. Nanotechnol., 2011, **6**, 147.

17 B. Radisavljevic, M. B. Whitwick, and A. Kis, ACS Nano, 2011, **5**, 9934.

18 B. Radisavljevic, M. B. Whitwick, and A. Kis, Appl. Phys. Lett., 2012, **101**, 043103.

19 Z. Y. Yin, H. Li, L. Jiang, Y. M. Shi, Y. H. Sun, G. Lu, Q. Zhang, X. D. Chen, and H. Zhang, ACS Nano, 2012, **6**, 74.

20 H. S. Lee, S.-W. Min, Y.-G. Chang, M. K. Park, T. Nam, H. Kim, J. H. Kim, S. Ryu, and S. Im, Nano Lett., 2012, **12**, 3695.

21 O. Lopez-Sanchez, D. Lembke, M. Kayci, A. Radenovic, and A. Kis, Nat. Nanotechnol., 2013, **8**, 497.

22 A. Splendiani, L. Sun, Y. Zhang, T. Li, J. Kim, C.-Y. Chim, G. Galli, and F. Wang, Nano Lett., 2010, **10**, 1271.

23 S. Tongay, H. Sahin, C. Ko, A. Luce, W. Fan, K. Liu, J. Zhou, Y.-S. Huang, C.-H. Ho, J. Yan, D. F. Ogletree, S. Aloni, J. Ji, S. Li, J. Li, F.M. Peeters, and J. Wu, Nature Commun., 2014, **5**, 3252.

24 S. Horzum, D. Cakir, J. Suh, S. Tongay, Y.-S. Huang, C.-H. Ho, J. Wu, H. Sahin, and F. M. Peeters, Phys. Rev. B, 2014, **89**, 155433.

25 S. Y. Hu, C. H. Liang, K. K. Tiong, Y. S. Huang, and Y. C. Leed, J. Electrochem. Soc., 2006, **153**, J100.

26 S. Y. Hu, S. C. Lin, K. K. Tiong, P. C. Yen, Y. S. Huang, C. H. Ho, and P.C. Liao, J. Alloys Compd., 2004, **383**, 63.

27 D. O. Dumcenco, Y. S. Huanga, C. H. Liang and K. K. Tiong, J.Appl.Phys., 2007, **102**, 083523.

28 K. K. Tiong, Y. S. Huang, and C. H. Ho, J. Alloys Compd., 2001, **317-318**, 208.

29 F. L. Deepak, R. Popovitz-Brio, Y. Feldman, H. Cohen, A. Enyashin, G. Seifert, and R. Tenne, Chem. Asian. J., 2008, **3**, 1568.

30 L. Rapoport, A. Moshkovich, V. Perfilyev, A. Laikhtman, I. Lapsker, L. Yadgarov, R. Rosentsveig, and R. Tenne, Tribol. Lett., 2012, **45**, 257.

31 V. V. Ivanovskaya, A. Zobelli, A. Gloter, N. Brun, V. Serin, and C. Colliex, Phys. Rev. B, 2008, **78**, 134104.

32 F. L. Deepak, H. Cohen, S. Cohen, Y. Feldman, R. Popovitz-Brio, D. Azulay, O. Millo, and R. Tenne, J. Am. Chem. Soc., 2007, **129**, 12549.

33 Y. Shi, J. K. Huang, L. Jin, Y. T. Hsu, S. F. Yu, L. J. Li, and H. Y. Yang, Sci. Rep., 2013, **3**, 1839.

34 G. Kresse and J. Hafner, Phys. Rev. B, 1993, **47**, 558.

35 G. Kresse and J. Furthmuller, Phys. Rev. B, 1996, **54**, 11169.

36 J. P. Perdew, K. Burke, and M. Ernzerhof, Phys. Rev. Lett., 1996, **77**, 3865.

37 G. Kresse and D. Joubert, Phys. Rev. B, 1999, **59**, 1758.

38 H. J. Monkhorst and J. D. Pack, Phys. Rev. B, 1976 **13**, 5188.

39 K. Momma and F. Izumi, J. Appl. Crystallogr., 2008, **41**, 653.

40 J. C. Wildervanck and F. Jellinek, J. Less-Common Met., 1971, **24**, 731781.

41 N. W. Alcock and A. Kjekshus, Acta Chem. Scand., 1965, **19**, 79.

42 H. P. Komsa and A. V. Krasheninnikov, J. Phys. Chem. Lett., 2012, **3**, 3652.

43 S. Furuseth and A. Kjekshus, Acta Chem. Scand., 1966, **20**, 245.

44 L. Yang, K. Majumdar, Y. Du, H. Liu, H. Wu, M. Hatzistergos, P. Hung, R. Tieckelmann, W. Tsai, C. Hobbs, P. D. Ye, arXiv:1406.4492 [cond-mat.mtrl-sci].

45 K. Dolui, I. Rungger, C. D. Pemmaraju, and S. Sanvito, Phys. Rev. B, 2013, **88**, 075420.

46 Y.-C. Lin, D. O. Dumcenco, H.-P. Komsa, Y. Niimi, A. V. Krasheninnikov, Y.-S. Huang, and K. Suenaga, Adv. Mater., 2014, DOI: 10.1002/adma.201304985.